Local inhomogeneity effects on a nucleation process in a high external bias

Takeo Kato*
Department of Applied Physics, Osaka City University, Sumiyoshi-ku, Osaka 558-8585, Japan
(Received 21 February 2001; published 11 September 2001)

Quantum-nucleation processes in the presence of local moderate inhomogeneities are studied theoretically at high biases, where the potential of the field can be approximated by a cubic polynomial. The quantum-nucleation rate Γ is calculated for one-dimensional systems in a form $\Gamma = A \exp(-B/\hbar)$ by using the ''bounce'' method without any reduction to a single-variable problem. The bias dependence of the exponent B is typically described as $B \sim (f_c - f)^{\gamma}$, where f and f_c are an external bias and a classical threshold bias, repectively. The exponent γ changes from 1 to 5/4 as the effective impurity strength $\tilde{\varepsilon}$ increases, where $\tilde{\varepsilon}$ depends not only on the bare impurity strength but also on the bias f. This change is explained by the reduction of the effective spatial dimension of the system. By studying the system-size dependence of the prefactor A, the condition for the appearance of inhomogeneity effects is evaluated. Nucleation rates in thermal activation regimes are also calculated, and compared with quantum-tunneling regimes. For higher-dimensional systems, it is shown that the local approximation of inhomogeneity does not hold, and that spatial profiles of inhomogeneity become important.

DOI: 10.1103/PhysRevB.64.134106 PACS number(s): 64.60.Qb, 03.65.Sq, 73.40.Gk

I. INTRODUCTION

Nucleation process is one of the most universal phenomena found in various areas in physics from cosmology to condensed-matter physics providing the mechanism for the onset of first-order transitions.[1] Besides classical nucleation due to thermal fluctuations, nucleation due to quantum tunneling has attracted interest for many years as macroscopic quantum phenomena. Although quantum nucleation has been studied theoretically in the pioneering issue,[2] it is just recently that observation of quantum nucleation has become possible owing to the progress in experimental techniques. At present, quantum nucleation has been observed experimentally in low-temperature condensed-matter systems: ^{4}He-^{3}He liquid solutions,[3,4] cavitation in ^{4}He liquid,[5] nucleation of ^{4}He solids.[6] Nucleation of magnetic domain in thin films has also been discussed theoretically.[7–9] Quantum creation of a kink-antikink pair can be regarded as one-dimensional nucleation, and has been studied both experimentally and theoretically in dislocation motion in solids,[10,11] and sliding of charge-density waves (CDW's),[12–17] though in the latter system interpretations of the experimental results are not settled.[18–20] I believe that long Josephson junctions[21–25] are also suitable to observe quantum nucleation of a soliton pair.

In many theoretical issues, nucleation processes have been restricted to the situation that a stable phase is formed in the otherwise *homogeneous* background of an unstable phase. In several literatures, the nucleation rates in the presence of strong inhomogeneities have also been studied by using a single-variable model.[26] In such studies, direct evaluation of the impurity strength from the nucleation rate is difficult, because the parameters of the single-variable model cannot be related clearly to the impurity strength. In this paper, we study *moderate* inhomogeneities, which can be controlled by an external parameter from the nearly homogeneous region to the strongly inhomogeneous region. This crossover region has not been studied in detail, and provides useful information of the impurity strength, because the nucleation rates are very sensitive to the impurity strength in this region.

In this paper, we study how the nucleation process changes in the presence of local moderate inhomogeneity. As a starting point, a highly biased region is investigated where the potential can be expressed by a cubic polynomial. The nucleation rate is calculated based on the ''bounce'' method[27–29] for quantum-tunneling regimes, and on Kramers' law for thermal activation regimes.[1,30] We concentrate on nucleation processes in one-dimensional systems that correspond to the kink-antikink nucleation. We show that extension to higher dimensions is not easy since the nucleation rates are affected by details of local inhomogeneity profiles such as an impurity size.

The nucleation rate is expressed in the form $\Gamma = A \times \exp(-B/\hbar)$, where A and B are called as a prefactor and an exponent, respectively. The exponent B depends on the bias f as

$$B \propto (f_c - f)^{\gamma}, \tag{1.1}$$

where f_c is a classical threshold bias at which the potential barrier disappears. It should be stressed that the value of γ is modified by inhomogeneities. The modification of γ has first been discussed in the quantum sliding of CDW's by Yumoto *et al.*[31–33] They have calculated the nucleation rate by reducing the model to a single-variable problem with use of path integrals, and have reported that the value of γ increases as the impurity strength is enlarged. This method, however, is so complicated that it is difficult to discuss the origin of the change of γ clearly, and also to examine the validity of the approximation adopted there. In this paper, we study inhomogeneity effects without any reduction to a single-variable problem. It is claimed that our results are explained by the ''dimensionality'' of nucleation, which has been pointed out by the author in Ref. 34.

We consider one isolated impurity in a system with the size L. The results obtained in this paper are also applicable to systems with the dilute impurities by taking the average-impurity distance as L. In the limit $L\to\infty$, nucleation occurs dominantly in homogeneous regions of the samples, and no impurity effects appear. The inhomogeneity effects appear only when L is below a crossover value $L_{\rm cr}$. Within the bounce method, $L_{\rm cr}$ is shown to be obtained by calculating the prefactor A. Here, we should note that the validity of the bounce method is not guaranteed generally for the many-body problems. We also discuss the validity of the bounce method when it is applied to the nucleation problem in the presence of the impurities.

This paper is organized as follows. The model Hamiltonian is given in Sec. II. The quantum-tunneling rate is formulated and calculated for one-dimensional systems in Sec. III. We study the thermal regime in Sec. IV briefly, and the extension to higher-dimensional systems and justification of the bounce method are discussed in Sec. V. Finally, results are summarized in Sec. VI.

II. MODEL

In this paper, nucleation rates are calculated based on the equation of motion

$$\phi_{tt}-\nabla^2\phi+\frac{\partial V}{\partial\phi}=0. \tag{2.1}$$

Here, $\phi(\vec{x},t)$ is a $(d+1)$-dimensional field, and x and t are scaled by the characteristic length and time, respectively. Dissipation is assumed to be weak enough, but not extremely weak so that the system is in a thermal equilibrium in a metastable well. We concentrate on one-dimensional systems described by the equation

$$\phi_{tt}-\phi_{xx}+\frac{\partial V}{\partial\phi}=0, \tag{2.2}$$

and the higher-dimensional systems are discussed only in Sec. V. The potential energy is assumed to consist of two parts as $V(\phi,x)=V_0(\phi)+V_{\rm imp}(\phi,x)$, where $V_0(\phi)$ is a homogeneous part and $V_{\rm imp}(\phi,x)$ describes an inhomogeneity.

As for the homogeneous part $V_0(\phi)$, we assume: (1) the potential has at least one metastable point ϕ_0; (2) the energy barrier in $V_0(\phi)$ is controlled by an external parameter such as an external field. One typical example for $V_0(\phi)$ is a tilted cosine potential

$$V_0(\phi)=(1-\cos\phi)-f\phi. \tag{2.3}$$

Another example is the ϕ^4 model with a bias

$$V_0(\phi)=-\frac{\phi^2}{2}+\frac{\phi^4}{4!}-f\phi. \tag{2.4}$$

The type in Eq. (2.3) has been used for long Josephson junctions, dislocation in solids, and CDW systems, while the type in Eq. (2.4) describes an effective model for nucleation of a stable phase from an unstable background.

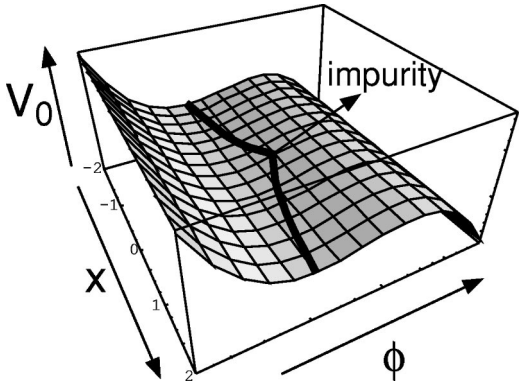

FIG. 1. String motion in the potential $V_0(\phi)$. The impurity effect is described by a local force for this string at $x=0$.

In this paper, the characteristic action of the systems is assumed to be large as compared with the Planck constant. In such situations, the quantum nucleation appears only when the bias f is controlled near the classical threshold f_c at which the metastable state of the potential $V_0(\phi)$ disappears. Note that $f_{\rm c,0}=1$ for the tilted cosine potential and $f_{\rm c,0}=2\sqrt{2}/3$ for the ϕ^4 model in the absence of impurities. Near $f=f_{\rm c,0}$, the potentials in Eqs. (2.3) and (2.4) form can be approximated commonly by quadratic-plus-cubic polynomials around a metastable point $\phi=\phi_0$ as

$$V_0(\phi)-V_0(\phi_0)\simeq\frac{a(f_{\rm c,0}-f)^{1/2}}{2}(\phi-\phi_0)^2-\frac{b}{6}(\phi-\phi_0)^3. \tag{2.5}$$

Here $a=O(1)$ and $b=O(1)$. To be explicit, $a=2^{1/2}$, $b=1$ for the tilted cosine potential (2.3), while $a=2^{3/4}$, $b=2^{1/2}$ for the ϕ^4 model (2.4).

The equation of motion (2.2) describes dynamics of a string in the potential $V(\phi)$ shown in Fig. 1. When the string is initially located in a metastable well, it stays there for a while, and then begins to move towards lower-energy states. If the system size is large enough, the transition from metastable states to moving states occurs through local deformation of the string accompanied with the creation of one kink-antikink pair. This transition can be regarded as ''nucleation'' when the metastable(stable) state is related to the metastable(stable) phase.

The local inhomogeneity is introduced by $V_{\rm imp}(\phi)$ as

$$V_{\rm imp}(\phi,x)=\delta(x)h(\phi), \tag{2.6}$$

where $\delta(x)$ is a delta function, and $h(\phi)$ is a function defined around the metastable point. This type of impurity potentials has been studied theoretically in CDW systems[31–33] and long Josephson junctions.[35,36] The potential form (2.6) can be obtained not only for impurities but also for inhomogeneities of external forces, modulation of barrier heights, and edge effects. (Details are summarized in the Appendix.) At high biases, since the impurity effect is determined by a small modulation of ϕ around the metastable point ϕ_0, the inhomogeneity potential can be approximated as

$$V_{\rm imp}(\phi,x)\sim-\varepsilon\,\delta(x)(\phi-\phi_0). \tag{2.7}$$

Here, ε describes the impurity strength. This local potential can be regarded as a local force on a string at $x=0$ as shown in Fig. 1. For $\varepsilon>0$ ($\varepsilon<0$), the string is attracted towards the positive(negative) direction of ϕ. As a result, the nucleation is enhanced around $x=0$ for $\varepsilon>0$, and suppressed for $\varepsilon<0$.

The appearance of the impurity effect is explained intuitively as follows. The nucleation rate Γ is expected to consist of two parts as $\Gamma=\Gamma_{\rm bulk}+\Gamma_{\rm imp}$. Here, $\Gamma_{\rm bulk}$ is the nucleation rate in the homogeneous region far from an impurity, and $\Gamma_{\rm imp}$ is a contribution near the impurity. Using the system size L, the bulk part is estimated as $\Gamma_{\rm bulk}\sim\Gamma_0 L$, where Γ_0 is the nucleation rate per unit length in the absence of the impurities. The impurity part $\Gamma_{\rm imp}$ is independent of L, and is estimated as $\Gamma_{\rm imp}\sim\Gamma_0\exp(\Delta U/\hbar\omega_0)$, where ΔU is the energy gain at the impurity site, and ω_0 is an attempt frequency around the metastable state. If the system size L is large enough, the bulk part $\Gamma_{\rm bulk}$ dominates the impurity part $\Gamma_{\rm imp}$, and no impurity effects appear. However, by controlling ΔU, $\Gamma_{\rm imp}$ can dominate $\Gamma_{\rm bulk}$. The inequality $\Gamma_{\rm imp}\gg\Gamma_{\rm bulk}$ leads

$$\Delta U\gg\hbar\omega_0\ln L. \tag{2.8}$$

Since the condition (2.8) shows a weak system-size dependence through the logarithmic function of L, it is expected to be feasible in experimental systems. The inequality (2.8), which can be derived more accurately in Sec. III D, will be assumed in the following section.

In this paper, we further assume $\varepsilon>0$ in Eq. (2.7), because $\Gamma_{\rm imp}$ never dominates the bulk part $\Gamma_{\rm bulk}$ in case of $\varepsilon<0$.

III. QUANTUM-TUNNELING REGIME

A. Formulation and scaling analysis

The quantum nucleation rate in the presence of the impurity is formulated by a semiclassical method as follows. The partition function of the system is expressed in terms of path integrals as

$$Z=\int\mathcal{D}\phi(x,\tau)\exp\left(-\frac{S[\phi(x,\tau)]}{\hbar}\right), \tag{3.1}$$

$$S[\phi(x,\tau)]=\int_{-L/2}^{L/2}dx\int_0^{\hbar\beta}d\tau\left[\frac{1}{2}\phi_x^2+\frac{1}{2}\phi_\tau^2+V_0(\phi)+V_{\rm imp}(x,\phi)\right], \tag{3.2}$$

where $\hbar$ is a dimensionless Planck constant normalized by the characteristic frequency, length, and energy of the system, $\tau=it$ is an imaginary time, and $\beta=1/k_{\rm B}T$ is an inverse temperature. The potential forms are given by Eqs. (2.5) and (2.7). By rescaling the variables as

$$x=x'(a\sqrt{f_{\rm c,0}-f})^{-1/2}, \tag{3.3}$$

$$\tau=\tau'(a\sqrt{f_{\rm c,0}-f})^{-1/2}, \tag{3.4}$$

$$\phi=\frac{a\sqrt{f_{\rm c,0}-f}}{b}\varphi+\phi_0, \tag{3.5}$$

the action is rewritten as

$$S[\varphi(x,\tau)]=\frac{a^2(f_{\rm c,0}-f)}{b^2}\int_{-\tilde{L}/2}^{\tilde{L}/2}dx'\int_0^{\hbar\tilde{\beta}}d\tau'\times\left[\frac{1}{2}\varphi_x^2+\frac{1}{2}\varphi_\tau^2+\frac{1}{2}\varphi^2-\frac{1}{3!}\varphi^3-\tilde{\varepsilon}\,\delta(x')\varphi\right]. \tag{3.6}$$

Here, $\tilde{L}=La^{1/2}(f_{\rm c,0}-f)^{1/4}$ and $\tilde{\beta}=\beta a^{1/2}(f_{\rm c,0}-f)^{1/4}$ is a scaled length and inverse temperature, respectively. The impurity effect is described only through an effective impurity strength $\tilde{\varepsilon}$ defined by

$$\tilde{\varepsilon}=\varepsilon a^{-3/2}b(f_{\rm c,0}-f)^{-3/4}. \tag{3.7}$$

This effective impurity strength depends on both the bare impurity strength ε and external bias f. Even if ε is fixed, we can control the strength of the impurity effect by changing the external current; the impurity effect is enhanced by controlling the external current near the threshold current f_c.

The partition function given in Eqs. (3.1) and (3.2) is evaluated by integrating the partition function around stationary solutions up to second-order fluctuations. The stationary solutions are determined by

$$\frac{\delta S}{\delta\varphi}=-\varphi_{\tau'\tau'}-\varphi_{x'x'}+\varphi-\frac{\varphi^2}{2}-\tilde{\varepsilon}\,\delta(x')=0. \tag{3.8}$$

There exist two types of solutions for this equation. One is a stable solution $\varphi_0(x')$ independent of τ', and the other is a ''bounce'' solution $\varphi_{\rm B}(x',\tau')$. Since the system has a metastable state, the free energy $F=-\beta^{-1}\ln Z$ gains an imaginary part. Then, the decay rates are given by $\Gamma=2\,{\rm Im}\,F$. This formula, derived through the ''bounce'' method, was first applied to the thermal-activation regime,[39,40] and extended to the quantum-tunneling regime.[2,27–29] The nucleation rate is now written in the form

$$\Gamma=A\exp(-B/\hbar), \tag{3.9}$$

and the exponent B and prefactor A are given as

$$B=S[\varphi_{\rm B}(x',\tau')]-S[\varphi_0(x')], \tag{3.10}$$

$$A=\frac{\overline{a}(T)}{\beta\hbar}\prod_{i=1}^{\infty}\left(\frac{|\lambda_i^{\rm (B)}|}{\lambda_i^{(0)}}\right)^{-1/2}. \tag{3.11}$$

Here, $\overline{a}(T)$ is a temperature-dependent factor, and takes 1 for $T<T_0$, and T_0/T for $T>T_0$[41], and $\lambda_i^{\rm (B)}$s ($\lambda_i^{(0)}$s) are the frequencies of eigenmodes around the bounce(stable) solution determined by the equation

$$[-\partial_{\tau'\tau'}-\partial_{x'x'}+1-\phi_{\rm B,0}(x',\tau')]\psi_i^{\rm (B,0)}(x',\tau')=\lambda_i^{\rm (B,0)}\psi_i^{\rm (B,0)}(x',\tau'). \tag{3.12}$$

All the eigenvalues around the stable solution are positive ($\lambda_i^{(0)}\geqslant 1$). The lowest eigenvalue $\lambda_1^{(B)}$ is negative due to the

metastability of the bounce solution $\varphi_{\rm B}$. The second-lowest eigenvalue $\lambda_2^{(B)}$ is always zero due to the translational symmetry of $\varphi_{\rm B}$ in the τ direction. This mode must be treated by the Fadeev-Popov method, and the expression of the prefactor is modified as[28,38]

$$\frac{1}{\sqrt{\lambda_2^{(B)}}} \to \sqrt{\frac{B}{2\pi\hbar}} \int_0^{\hbar\tilde{\beta}} d\tau_0', \tag{3.13}$$

where τ_0' denotes the center position of the bounce. For the weak impurity, the third eigenvalue $\lambda_3^{(B)}$ also approaches zero due to the translational symmetry of $\varphi_{\rm B}$ in the x direction. We study this mode in Sec. III D in detail.

B. Dimensional crossover

The bias dependence of the exponent B can be discussed from the viewpoint of the ''dimensional crossover.'' This viewpoint has been discussed in several physical systems such as CDW's,[17] and long Josephson junctions[37] in the context of the system-size dependences. The application to impurity problems has been discussed recently in Ref. 34. Here, we briefly summarize this viewpoint.

For the weak impurity $\tilde{\varepsilon} \ll 1$, the bias dependence of the exponent B is obtained as

$$B \propto (f_{\rm c,0} - f)^{3/2-(d+1)/4}. \tag{3.14}$$

Note that the exponent of $(f_{\rm c,0}-f)$ depends crucially on the spatial dimension d. The factor 3/2 comes from the bias dependence of the barrier height $\Delta U \propto (f_{\rm c,0}-f)^{3/2}$, while the factor $-(d+1)/4$ comes from the fact that the typical size of the bounce solution in the spatial(temporal) coordinates is given by $(f_{\rm c,0}-f)^{-1/4}$ for each of original coordinates $(x,\ \tau)$. [See Eqs. (3.3) and (3.4).]

The impurity effect can be explained by the change in the dimension: the strong impurity changes the spatial dimensionality d to zero. The classical threshold bias is also modified from $f_{\rm c,0}$ to $f_{\rm c}$. As a result, the bias dependence of B becomes

$$B \propto (f_c - f)^{3/2-1/4} = (f_c - f)^{5/4} \tag{3.15}$$

in the presence of strong impurities. In this region, the nucleation process is well described by a local deformation of the field, and is reduced to a one-variable problem.

This viewpoint is valid in the one-dimensional case as shown in the subsequent sections. In the $d \geqslant 2$ case, however, the viewpoint of the dimensional crossover in this paper cannot be discussed, since the impurity potential cannot be described by the delta function in Eq. (2.7), as will be discussed in Sec. V.

C. Exponent

For one-dimensional systems, the exponent B is calculated in a form $B=\sigma\tilde{B}(\tilde{\varepsilon})$. The factor $\sigma = a^2(f_c-f)/b^2$ describes the bias dependence in the absence of the impurities, while the scaled exponent $\tilde{B}(\varepsilon)$ is calculated as

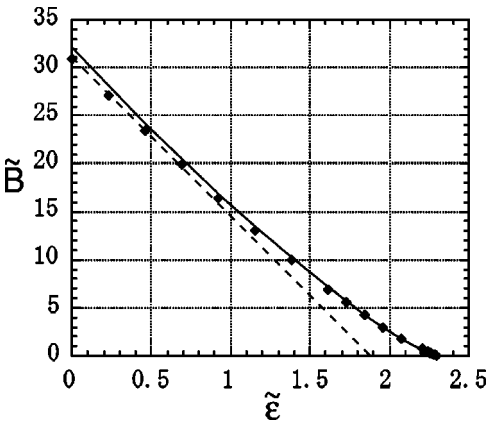

FIG. 2. The scaled exponent $\tilde{B}(\tilde{\varepsilon})$ as a function of the effective impurity $\tilde{\varepsilon}$. The numerical result is shown by the square dots. Dashed and solid lines corresponds to the analytical results for the weak impurities (3.19) and for the strong impurities (3.28), respectively.

$$\tilde{B}(\tilde{\varepsilon}) = \tilde{S}[\varphi_{\rm B}(x',\tau')] - \tilde{S}[\varphi_0(x')], \tag{3.16}$$

$$\tilde{S}[\varphi(x',\tau')] = \int_{-\tilde{L}/2}^{\tilde{L}/2} dx' \int_0^{\hbar\tilde{\beta}} d\tau' \left[\frac{1}{2}\varphi_{x'}^2 + \frac{1}{2}\varphi_{\tau'}^2 + \frac{1}{2}\varphi^2 - \frac{1}{6}\varphi^3 - \tilde{\varepsilon}\,\delta(x')\varphi \right]. \tag{3.17}$$

The impurity effect appears only through $\tilde{B}(\tilde{\varepsilon})$. In the homogeneous case, $\tilde{B}(\tilde{\varepsilon})$ is obtained as

$$\tilde{B}(0) = \tilde{S}[\varphi_{\rm B}(x',\tau';\tilde{\varepsilon}=0)] = 31.00, \tag{3.18}$$

and the exponent behaves as $B=\tilde{B}(0)\sigma \propto (f_c-f)^1$. As the effective impurity strength $\tilde{\varepsilon}$ increases, $\tilde{B}(\tilde{\varepsilon})$ is suppressed, and the tunneling rate is enhanced. At a critical value $\tilde{\varepsilon}_{\rm cl} = 4/\sqrt{3} \simeq 2.31$, the potential barrier disappears, and the exponent B is reduced to zero. Note that before the exponent B becomes zero, the bounce method becomes invalid because it is justified only in the semiclassical condition $B/\hbar \gg 1$. However, the region where the bounce method is broken down is narrow since the normalized Planck constant $\hbar$ is assumed to be small enough.

We calculate the function $\tilde{B}(\tilde{\varepsilon})$ by solving the equation (3.8) numerically. The Newton method is used by dividing the x'-τ' $(x'>0,\ \tau'>0)$ space into 64×64 cells. The result is shown in Fig. 2 by square dots.

Analytical expressions of $\tilde{B}(\tilde{\varepsilon})$ can be obtained in the limiting cases.[34] For the weak impurity $(\tilde{\varepsilon} \ll 1)$, $\tilde{B}(\tilde{\varepsilon})$ is evaluated by using the bounce solution in the homogeneous case $\tilde{\varepsilon}=0$ as

$$\tilde{B}(\tilde{\varepsilon}) = \tilde{S}_0 - \tilde{\varepsilon}\int_{-\infty}^{\infty} d\tau'\,\varphi_{\rm B}(0,\tau';\tilde{\varepsilon}=0) + O(\tilde{\varepsilon}^2)$$

$$= 31.00 - 16.43\tilde{\varepsilon} + O(\tilde{\varepsilon}^2). \tag{3.19}$$

This result is shown in Fig. 2 by the dashed line.

For the strong impurity $\tilde{\varepsilon}\sim\tilde{\varepsilon}_{\rm cl}$, the local modulation of the field becomes relevant, and a one-mode approximation is effective. We first evaluate the solutions of Eq. (3.8) for $\tilde{\varepsilon}=\tilde{\varepsilon}_{\rm cl}$. The bounce solution $\varphi_{\rm B}(x')$ agrees with the stable solution $\varphi_0(x')$, and is obtained analytically as

$$\varphi_{\rm B}(x';\tilde{\varepsilon}_{\rm cl})=\frac{3}{\cosh^2[(x'+a_{\rm cl})/2]}, \tag{3.20}$$

where $\tanh(a_{\rm cl}/2)=1/\sqrt{3}$. At the critical point $\tilde{\varepsilon}=\tilde{\varepsilon}_{\rm cl}$, there appears the zero-frequency mode ($\lambda_1^{(B)}=0$) around the solution $\varphi_{\rm B}(x;\tilde{\varepsilon}_{\rm cl})$. The eigenfunction of this mode is obtained from Eq. (3.12) as

$$\psi_1^{(B)}(x';\tilde{\varepsilon})=\frac{C\sinh[(x'+a_{\rm cl})/2]}{\cosh^3[(x'+a_{\rm cl})/2]}, \tag{3.21}$$

where C is a normalization factor determined from $\int|\psi_1^{(B)}|^2dx'=1$, and is given by

$$C=\sqrt{\frac{135}{8(9-2\sqrt{3})}}\simeq 1.746. \tag{3.22}$$

When $\tilde{\varepsilon}$ is slightly smaller than $\tilde{\varepsilon}_{\rm cl}$, this mode describes slow dynamics of the system, and is related to the tunneling process. Hence, we can approximate the bounce solution as

$$\varphi_{\rm B}(x',\tau';\tilde{\varepsilon})\simeq\varphi_{\rm B}(x';\tilde{\varepsilon}_{\rm cl})+X(\tau')\psi_1^{(\rm B)}(x'), \tag{3.23}$$

where $X(\tau')$ is a tunneling variable denoting the dynamics of the local deformation at the impurity site. By substituting Eq. (3.23) into the action (3.17), we obtain the action in terms of $X(\tau')$ as

$$\tilde{S}[X(\tau')]=\int_0^{\hbar\tilde{\beta}}d\tau'\left[\frac{1}{2}\left(\frac{dX}{d\tau'}\right)^2+V(X)\right] \tag{3.24}$$

$$V(X)=\frac{2\sqrt{3}}{9}(\tilde{\varepsilon}_{\rm cl}-\tilde{\varepsilon})CX-\frac{4}{243}(CX)^3. \tag{3.25}$$

This action corresponds to one-particle dynamics in a cubic potential $V(X)$. The potential barrier ΔU and frequency of small oscillation around the metastable state ω_0 are given as

$$\Delta U=2^{5/2}\times 3^{-5/4}(\tilde{\varepsilon}_{\rm cl}-\tilde{\varepsilon})^{3/2} \tag{3.26}$$

$$\omega_0=2^{5/4}\times 3^{-11/8}C(\tilde{\varepsilon}_{\rm cl}-\tilde{\varepsilon})^{1/4}. \tag{3.27}$$

By applying the standard bounce technique[27,29] to this potential, the function $\tilde{B}(\tilde{\varepsilon})$ is obtained

$$\tilde{B}(\tilde{\varepsilon})=\frac{36\Delta U}{5\hbar\omega_0}\simeq 11.25(\tilde{\varepsilon}_{\rm cl}-\tilde{\varepsilon})^{5/4}. \tag{3.28}$$

This result, shown in Fig. 2 by a solid line, agrees with the numerical result for the strong impurity strength, and gives a good estimate even for the weak impurity. The expression (3.28) may be useful to analyze experimental data.

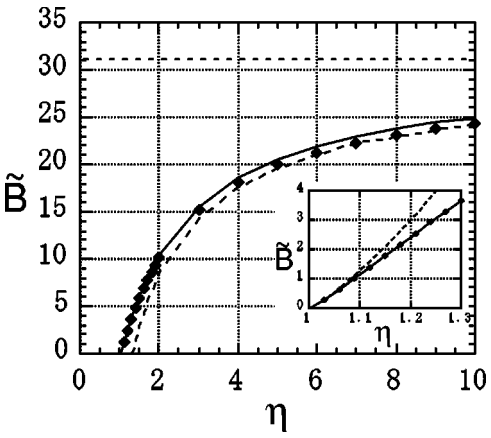

FIG. 3. The scaled exponent $\tilde{B}$ versus the bias parameter $\eta=(f_{\rm c,0}-f)/(f_{\rm c,0}-f_c)$. The numerical results are shown by squares. Dashed and solid curves correspond to the analytical result for the weak impurity (3.19) and for the strong impurity (3.28), respectively. The horizontal dotted line shows the homogeneous case $\varepsilon=0$. The solid and dashed curves in the inset show the behavior of $\tilde{B}$ near the threshold bias $\eta=1$, and the asymptotic form (3.29) around $\eta=1$, respectively.

In order to analyze experimental results, it is convenient to draw the graph of $\tilde{B}(\tilde{\varepsilon})$. The feature of impurity effects can be obtained by this analysis. Concerning the highly biased region, this plot is universal in the sense that it does not depend on the bare impurity strength ε.

In order to apply the viewpoint of the dimensional crossover, the bias dependence of the exponent $\tilde{B}$ is discussed. For simplicity, the cosine potential with a bias term (2.3) is considered with a notation $f_{\rm c,0}=1$, [see above Eq. (2.5)] $a=\sqrt{2}$, $b=1$ [see below Eq. (2.5)]. We use the bias parameter $\eta=(f_{\rm c,0}-f)/(f_{\rm c,0}-f_{\rm c})$. It takes 0 and 1 corresponding the classical threshold ($f=f_{\rm c,0}=1$) in the absence of the impurities and to the critical bias ($f=f_c$) in the presence of the impurities, respectively. Here, $f_{\rm c}$ is defined by $\tilde{\varepsilon}_{\rm cl}=4/\sqrt{3}=\varepsilon(2(1-f_{\rm c}))^{-3/4}$. The graph of $\tilde{B}$ as a function of η is shown in Fig. 3. The numerical result is shown by square dots. Analytical results for the weak and strong impurities are also shown by the dashed and solid curves, respectively.

The dimensional crossover discussed in Sec. III B can be clarified in this figure. In the region $\eta\gg 1$ where the effective impurity strength $\tilde{\varepsilon}$ becomes small, $\tilde{B}$ becomes almost independent of the bias as seen in Fig. 3, and the exponent B behaves as $B\propto(f_{\rm c,0}-f)^1$ as expected in Eq. (3.14). As η approaches the critical threshold $\eta=1$, the effective impurity strength is enhanced, and the exponent is suppressed. The analytical expression near $\eta=1$ is obtained from Eq. (3.28) as

$$B\simeq 22.36(\eta-1)^{5/4}. \tag{3.29}$$

Hence, the exponent behaves as $B\propto(f_c-f)^{5/4}$ as expected in Eq. (3.15). We show the bias dependences near $\eta=1$ in the inset of Fig. 3. The exponent, thus, behaves as $B\propto(f_c-f)^{3/2-(d+1)/4}$, and the spatial dimension d seems to be re-

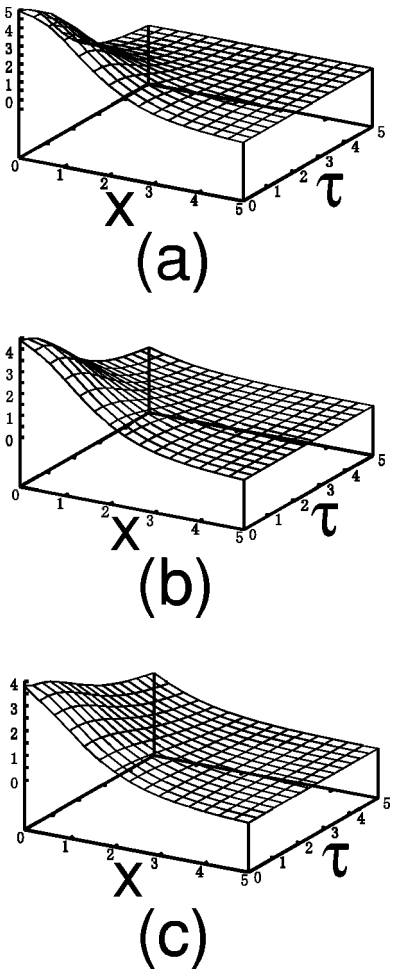

FIG. 4. Bounce solution for (a) $\tilde{\varepsilon}=0$, (b) $\tilde{\varepsilon}=1.24$, (c) $\tilde{\varepsilon}=1.98$. The critical value at the threshold bias is $\tilde{\varepsilon}=4/\sqrt{3}=2.31$.

duced to zero by the strong impurities accompanied with the change of the classical threshold f_c.

Finally, we show the bounce solution $\varphi_{\mathrm{B}}(x,\tau)$ in Fig. 4 in the region $x>0$, $\tau>0$. Note that the bounce solution has a reversal symmetry $\varphi_{\mathrm{B}}(x,\tau)=\varphi_{\mathrm{B}}(-x,\tau)=\varphi_{\mathrm{B}}(x,-\tau)$. The bounce solution is expected to describe the feature of the nucleation process; $\varphi(x,\tau)$ describes the shape of the field variable φ at the imaginary time τ. As the effective impurity strength increases, the boundary condition for the bounce solution $\varphi_{\mathrm{B}}(x,\pm\infty)=\varphi_0(x)$ is modified at the impurity site. As seen in Fig. 4, the nucleation process occurs only at the small region near the impurity site for the strong impurities. This change of the nucleation process is responsible for the qualitative difference between the weak and strong impurities.

D. Prefactor

The prefactor A is ordinarily a minor factor that is hard to be measured experimentally. However, it describes the system-size L dependence of the nucleation rate, which may be observed. Here, we study the prefactor A analytically in the limiting cases within the bounce method, and discuss the L dependence of the nucleation rate.

The prefactor is formulated in Eq. (3.11) with the improvement (3.13) due to the zero mode ($\lambda_2^{(B)}=0$). In the absence of the impurities, not only the second but also the third-lowest modes become the zero modes ($\lambda_3^{(B)}=0$), which need to be treated by the Fadeev-Popov method as

$$\frac{1}{\sqrt{\lambda_3^{(B)}}}\to\sqrt{\frac{\sigma\tilde{B}(0)}{2\pi}}\int_{-\tilde{L}/2}^{\tilde{L}/2}dx_0', \tag{3.30}$$

where x_0' denotes a position of the bounce center. This treatment gives the correct system-size dependence, $\Gamma\propto L$.

As for the weak impurity, the frequency of the third-lowest mode is lifted to a small positive frequency. Also in this case, the replacement in Eq. (3.30) is needed in order to obtain the correct system-size dependence. As a result, the tunneling rate is calculated as

$$\Gamma=\Gamma_0\left[\tilde{L}+\int_{-\tilde{L}/2}^{\tilde{L}/2}dx_0'(e^{\sigma\tilde{\varepsilon}f(x_0')}-1)\right], \tag{3.31}$$

where Γ_0 is the nucleation rate per unit length in the absence of the impurities, and the function $f(x_0')$ is defined by

$$f(x_0')=\int_{-\infty}^{\infty}d\tau'\,\varphi_{\mathrm{B}}(x_0',\tau';\tilde{\varepsilon}=0). \tag{3.32}$$

From this expression, the tunneling rate can be divided into two parts as

$$\Gamma_{\mathrm{bulk}}=\Gamma_0\tilde{L}, \tag{3.33}$$

$$\Gamma_{\mathrm{imp}}=\Gamma_0\int_{-\tilde{L}/2}^{\tilde{L}/2}dx_0'(e^{\sigma\tilde{\varepsilon}f(x_0')}-1). \tag{3.34}$$

The bulk part Γ_{bulk} is proportional to the system size $\tilde{L}$, while the impurity part Γ_{imp} is independent of the system size for $\tilde{L}\gg 1$.

Within the bounce method, the L dependence is naturally described as follows. For large L, Γ_{bulk} alway dominates Γ_{imp}, and no impurity effects appear. As L is reduced, the bulk part is suppressed, and below a crossover length $\tilde{L}_{\mathrm{cr}}$, the impurity part may overcome the bulk part. Only in this region, the impurity effect is clearly observed experimentally. The ratio $\Gamma_{\mathrm{imp}}/\Gamma_{\mathrm{bulk}}$ is determined by the scaled length $\tilde{L}$ and the impurity factor $\sigma\tilde{\varepsilon}$ in Eq. (3.34). For $\tilde{L}\gg 1$, the crossover length $\tilde{L}_{\mathrm{cr}}$ can be obtained as a function of $\sigma\tilde{\varepsilon}$ by taking the ratio as $\Gamma_{\mathrm{imp}}/\Gamma_{\mathrm{bulk}}=1$. Thus, the phase diagram is obtained by Fig. 5, where the crossover length is shown by the solid curve. In the upper region of the phase diagram, the nucleation occurs dominantly in the bulk region, while in the lower region, the impurity part dominates the bulk part, and inhomogeneity effects appear clearly.

The intuitive discussion about the appearance of the impurity effect in Sec. II can be now clarified in detail. The asymptotic form of the crossover length $\tilde{L}_{\mathrm{cr}}$ for $\sigma\tilde{\varepsilon}\gg 1$ is obtained analytically by applying the stationary method to the integral (3.34) as

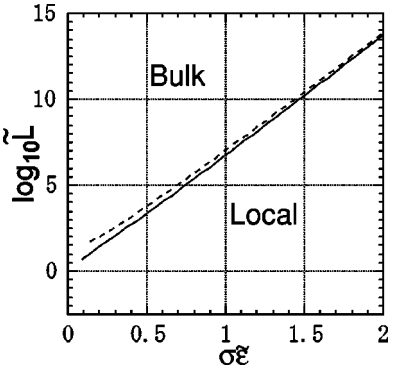

FIG. 5. Crossover length $\tilde{L}_{\rm cr}=L_{\rm cr}a^{1/2}(f_c-f)^{1/4}$ versus $\tilde{\varepsilon}\sigma=\varepsilon a^{1/2}(f_c-f)^{1/4}/b$. In the region $\tilde{L}>\tilde{L}_{\rm cr}$, nucleation occurs in the bulk region, while in the region $\tilde{L}<\tilde{L}_{\rm cr}$, the impurity contribution $\Gamma_{\rm imp}$ becomes dominant. The solid and dashed lines show the result and, the asymptotic expression (3.35) valid in the limit $\sigma\tilde{\varepsilon}\gg 1$, respectively.

$$\ln\tilde{L}_{\rm cr}\simeq 16.43(\sigma\tilde{\varepsilon})-0.211-\tfrac{1}{2}\ln(\sigma\tilde{\varepsilon}). \tag{3.35}$$

This result is shown in Fig. 5 by the dashed curve. The predominant term in Eq. (3.35) can be related to the enhancement of the exponent ΔB defined by

$$\Delta B=\sigma\tilde{\varepsilon}\int_{-\infty}^{\infty}d\tau'\,\varphi_{\rm B}(x=0,\tau';\tilde{\varepsilon}=0), \tag{3.36}$$

as $\ln\tilde{L}_{\rm cr}=\Delta B$. Since ΔB is estimated by the local suppression of the potential barrier ΔU and the typical attempt frequency ω_0 as $\Delta B\sim\Delta U/\hbar\omega_0$, the expression in Eq. (2.8) can be reproduced qualitatively.

Beyond the perturbational analysis of $\tilde{\varepsilon}$, it is difficult to calculate the prefactor, because the low-frequency modes may couple with each other. It would be a future problem to consider the nucleation rates in this regime. (See also Sec. V B.) Only for strong impurity, the prefactor can be calculated by assuming $\tilde{L}\ll\tilde{L}_{\rm cr}$ and by applying standard procedures[27,29,38] to one-variable problem (3.24) with Eq. (3.25) as

$$A\sim\sqrt{60}\sqrt{\frac{\tilde{B}(0)}{2\pi}}, \tag{3.37}$$

although the crossover length $\tilde{L}_{\rm cr}$ cannot be easily obtained even in this case.

IV. THERMAL-ACTIVATION REGIME

At high temperatures, nucleation is caused by thermal fluctuations. Since the nucleation rate has already been studied in this region in Ref. 34, we only summarize the feature of the impurity effect.

In the thermal activation regime, the nucleation rate is evaluated by Kramers' formula

$$\Gamma=A\exp(-\Delta U/k_{\rm B}T). \tag{4.1}$$

The potential barrier ΔU is calculated as

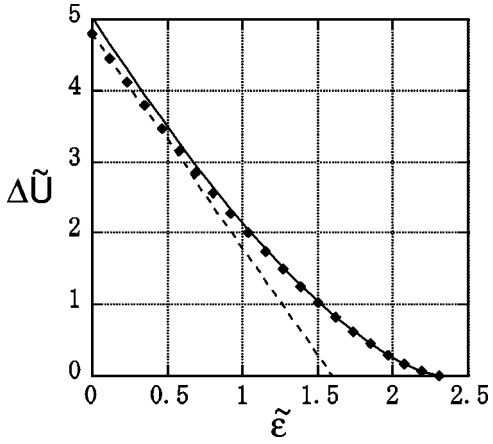

FIG. 6. The normalized barrier height $\Delta\tilde{U}$ versus the effective impurity strength $\tilde{\varepsilon}$. The numerical results are shown by square, while analytical results in the limiting case, (4.6) and (4.7), are shown by the dashed and solid curves, respectively.

$$\Delta U=U[\varphi_B(x')]-U[\varphi_0(x')], \tag{4.2}$$

$$U[\varphi(x')]=\frac{a^{5/2}(f_c-f)^{5/4}}{b^2}\int_{-\tilde{L}/2}^{\tilde{L}/2}dx' \times\left(\tfrac{1}{2}\varphi_{x'}^2+\tfrac{1}{2}\varphi^2-\tfrac{1}{6}\varphi^3-\tilde{\varepsilon}\,\delta(x')\varphi(x')\right). \tag{4.3}$$

Here, $\varphi_0(x')$ $[\varphi_{\rm B}(x')]$ is the stable (unstable) stationary solution satisfying

$$\frac{\delta U}{\delta\varphi(x')}=-\varphi_{x'x'}+\varphi-\frac{\varphi^2}{2}-\tilde{\varepsilon}\,\delta(x')=0. \tag{4.4}$$

The same result can be derived by applying the bounce method to a finite-temperature region.[39–43] Within the bounce method, the feature at high temperatures is explained as follows. At high temperatures, the bounce solution becomes independent of τ', since the interval in the τ direction becomes short. It means that the temporal dimension become irrelevant. Hence, the relevant dimension of the bounce is reduced from $(d+1)$ to d. Except for the absence of the temporal dimension, we can discuss the dimensional crossover in the same way as Sec. III B: the energy barrier behaves as $\Delta U\propto(f_c-f)^{5/4}$ for the weak impurity, while as $\Delta U\propto(f_c-f)^{3/2}$ for the strong impurity.

The barrier height is calculated in a form

$$\Delta U=\frac{a^{5/2}(f_c-f)^{5/4}}{b^2}\Delta\tilde{U}(\tilde{\varepsilon}). \tag{4.5}$$

The impurity effects appear only through the normalized potential barrier $\Delta\tilde{U}$. We show $\Delta\tilde{U}$ as a function of the effective impurity strength $\tilde{\varepsilon}$ in Fig. 6 by squares. The critical impurity strength is given by $\tilde{\varepsilon}_{\rm cl}=4/\sqrt{3}$ that is the same as

the quantum-tunneling regime. The exponent is obtained analytically for the weak impurity $\tilde{\varepsilon} \ll 1$ as

$$\Delta \tilde{U}(\tilde{\varepsilon}) = 24/5 - 3\tilde{\varepsilon}, \tag{4.6}$$

while for the strong impurity $\tilde{\varepsilon} \sim \tilde{\varepsilon}_{\rm cl}$ as

$$\Delta \tilde{U}(\tilde{\varepsilon}) = 1.433(\tilde{\varepsilon}_{\rm cl} - \tilde{\varepsilon})^{3/2}. \tag{4.7}$$

These results are shown in Fig. 6 by the dashed and solid curves. The feature of the impurity effect is the same as the zero-temperature case shown in Fig. 2.

V. DISCUSSION

A. Extension to the $d \geqslant 2$ case

First, let us discuss the two-dimensional systems. The stable solution $\varphi_0(x',y')$ is determined by

$$\varphi_{x'x'} + \varphi_{y'y'} = \varphi - \frac{1}{2}\varphi^2 - \tilde{\varepsilon}\,\delta(x')\,\delta(y'), \tag{5.1}$$

where the last term describes the impurity located at $(x',y')=0$. For the stationary solution having a rotational symmetry around the origin $(x',y')=(0,0)$, this equation is reduced, by using the radius coordinate $r=\sqrt{x'^2+y'^2}$, to

$$\frac{1}{r}\frac{\partial}{\partial r}\left(r\frac{\partial \varphi}{\partial r}\right) = \varphi - \frac{1}{2}\varphi^2 - \tilde{\varepsilon} g(r). \tag{5.2}$$

Here, $g(r)$ is a modified delta function satisfying $g(r)=0$ for $r>0$, $g(r)=\infty$ for $r=0$, and

$$\int_0^\infty dr\, 2\pi r g(r) = 1. \tag{5.3}$$

From Eqs. (5.2) and (5.3), the boundary condition at $r=0$ is obtained as

$$\lim_{r\to 0} r\frac{\partial \varphi}{\partial r} = -\frac{\tilde{\varepsilon}}{2\pi}. \tag{5.4}$$

Since the function $r\varphi_r$ is a continuous function at $r>0$, if we take an arbitrary constant A $(<\tilde{\varepsilon}/2\pi)$, there exists a constant a, and for all r in the range $0<r\leqslant a$

$$r\frac{\partial \varphi}{\partial r} \leqslant -A \tag{5.5}$$

is satisfied. As a result, $\varphi(r)$ is evaluated for $0<r<a$ as

$$\varphi(r) \geqslant A \ln\left(\frac{a}{r}\right) + \varphi(a), \tag{5.6}$$

and the value of φ diverges at $r=0$. Since φ must be finite in the present model, this divergence means that the local inhomogeneity cannot be described by the delta function in the two-dimensional systems. In other words, if we approximate the delta function as $g(r)=1/\pi r_0^2$ for $0<r<r_0$ and as $g(r)=0$ for $r_0<r$, the value of $\varphi(0)$ depends crucially on the impurity size r_0, and diverges in the limit $r_0 \to 0$. Also in the $d=3$ case, the field $\varphi(r)$ diverges at $r=0$, since the bounce solution behaves $\varphi(r) \propto 1/r$ near $r=0$, where $r=\sqrt{x'^2+y'^2+z'^2}$,

These results indicate that in the highly biased region, the system is sensitive to local inhomogeneities. To clarify the inhomogeneity effects in the $d \geqslant 2$ case, it is needed to consider the detailed profiles of the inhomogeneities beyond the local approximation adopted in this paper.

B. Validity of the bounce method

In this paper, the nucleation rate is calculated by the bounce method. Although this method has been applied to multivariable tunneling problems for many years, we should be careful of its validity. In principle, the exact tunneling rate should be determined by the full information about the action $S[\phi(x')]$. The bounce solution can extract important informations from the action; the exponent B is a difference of the action between the bounce and stable solutions, while the prefactor A is determined by the second-order fluctuations around both the solutions. While the bounce method is a convenient method to evaluate the tunneling rate, some informations that may affect the tunneling rate are dropped.

It is expected that the bounce method can be justified in the following conditions:[38] (1) we can define the tunneling variable describing slow dynamics among the many degrees of freedom, and (2) this tunneling variable is well separated from the other variables with fast dynamics. In these conditions, the system can be reduced to the one-variable tunneling problem where the bounce method is justified well. Here, let us consider the model adopted in this paper. For the strong impurity, it has been shown that the single-mode approximation gives a good estimate of the exponent B. In this region, the bounce method is expected to give correct results for both the exponent and the prefactor for $L \ll L_{\rm cr}$, though the crossover length $L_{\rm cr}$ itself cannot be evaluated. For the moderate impurity, however, there appears another low-frequency mode related to the Goldstone mode. This low-frequency mode is expected to couple with the tunneling mode. Hence, the bounce method may give an incorrect result especially for the prefactor determined only by the information about second-order fluctuations. It is a future problem to improve the bounce method in this situation.

VI. SUMMARY

The local inhomogeneity effects on nucleation processes have been studied within the bounce method at high biases. The nucleation rate has been calculated in a form $\Gamma = A\exp(-B/\hbar)$. It has been found that the effective impurity strength $\tilde{\varepsilon}$ can be controlled not only by the bare impurity strength ε but also by the external bias f. The exponent B has been calculated as a function of the effective impurity strength $\tilde{\varepsilon}$ without reduction to a single-variable tunneling problem. It has been shown that these results are well reproduced for the weak impurity by a perturbational analysis and for the strong impurity by a one-mode approximation. It has been clarified that the results can be explained by the reduction of the effective dimensionality of the system due to the

impurity. By calculating the prefactor A, the condition of the appearance of the impurity effects has been discussed and the phase diagram has been obtained.

There remain future problems. One of them is to study the inhomogeneity effect in higher-dimensional systems. As discussed in Sec. V, the local approximation does not hold for the $d \geqslant 2$ case. From this result, it is conjectured that the sample inhomogeneities may become essentially important for higher-dimensional systems. I think that the study of the inhomogeneity effects in high-dimensional systems would give an important aspect about the interplay of quantum tunneling and randomness.

ACKNOWLEDGMENT

I wish to acknowledge M. Yumoto for suggestions and helpful discussions.

APPENDIX: RELEVANCE OF THE LOCAL IMPURITY MODEL TO EXPERIMENTAL SYSTEMS

In this paper, the inhomogeneity effect is described by the potential

$$V_{\mathrm{imp}}(x,\phi)=\varepsilon(x)h(\phi). \tag{A1}$$

If the function $\varepsilon(x)$ changes only in a narrow region at the impurity site compared with the typical length scale $[\sim a^{-1/2}(f-f_c)^{-1/4}]$, it can be replaced with the delta function $\delta(x)$ in Eq. (2.6). The potential form (A1) can be realized in various experimental situations. One typical example is a spatial inhomogeneity of the bias. If the bias is assumed not to be uniform but to have a spatial dependence as $f+\varepsilon(x)$, then we have the potential form (A1). Another example is the inhomogeneity of the amplitude of the potential barrier in $V_0(\phi)$. If we replace, for example, the cosine potential in Eq. (2.3) with $[1+\varepsilon(x)](1-\cos\phi)$, then the form (A1) is also obtained. As for the Josephson junction systems, the coupling to the derivative of the field $\phi_x(x)$ can also be introduced by applying the magnetic field.[25] If the coupling is denoted with $b(x)\phi_x(x)$, the potential form (A1) is derived by taking the function $\varepsilon(x)$ as $-b_x(x)$.

In addition to the above situations, boundaries play a role of local inhomogeneities. The potential barrier ΔU is reduced to $\Delta U/2$ at open edge. Hence, the nucleation occurs dominantly at the boundary. The prefactor A of the nucleation rate is always independent of the system size, while the exponent B is affected by the boundary condition. Assuming that the field $\varphi(x')$ is defined at $x' \geqslant 0$, and that the boundary condition is given as

$$\varphi_{x'}(x'=0)=h, \tag{A2}$$

it can be shown easily that this boundary effect corresponds to the local inhomogeneity by taking $\tilde{\varepsilon}=2h$. Thus, the exponent B_{edge} is obtained as

$$B_{\mathrm{edge}}=\frac{1}{2}\sigma\tilde{B}(\tilde{\varepsilon}=2h). \tag{A3}$$

By changing the boundary condition at the edge, the impurity effects on the exponent can also be observed. Actually, this tendency has been observed in experiments.[23]

*Email address: kato@a-phys.eng.osaka-cu.ac.jp

[1] P. Hänngi, P. Talkner, and M. Borkovec, Rev. Mod. Phys. **62**, 251 (1990).
[2] I. M. Lifshitz and Yu. Kagan, Zh. Éksp. Teor. Fiz. **62**, 385 (1972) [Sov. Phys. JETP **35**, 206 (1972)].
[3] T. Satoh, M. Morishita, M. Ogata, A. Savada, and T. Kuroda, Physica B **169**, 513 (1991).
[4] T. Satoh, M. Morishita, M. Ogata, and S. Katoh, Phys. Rev. Lett. **69**, 335 (1992).
[5] S. Balibar, C. Guthmann, H. Lambare, P. Roche, E. Rolley, and H. J. Maris, J. Low Temp. Phys. **101**, 271 (1995).
[6] J. P. Ruutu, P. J. Hakonen, J. S. Penttilä, A. V. Bobkin, J. P. Saramäki, and E. B. Sonin, Phys. Rev. B **77**, 2514 (1996).
[7] A. O. Caldeira and K. Furuya, J. Phys. C **21**, 1227 (1988).
[8] E. M. Chudnovsky and L. Gunther, Phys. Rev. B **37**, 9455 (1988).
[9] E. M. Chudnovsky and J. Tejada, *Macroscopic Quantum Tunneling of the Magnetic Moment* (Cambridge University Press, Cambridge, 1998).
[10] S. Takeuchi, T. Suzuki, and H. Koizumi, J. Phys. Soc. Jpn. **69**, 1727 (2000).
[11] B. V. Petukhov, H. Koizumi, and T. Suzuki, Philos. Mag. A **77**, 1041 (1998).
[12] K. Maki, Phys. Rev. B **18**, 1641 (1978).
[13] K. Hida and U. Eckern, Phys. Rev. B **30**, 4096 (1984).
[14] S. Nakaya and K. Hida, J. Phys. Soc. Jpn. **55**, 3768 (1986).
[15] Ji-Min Duan, Phys. Rev. B **48**, 4860 (1993).
[16] K. Maki, Phys. Lett. A **202**, 313 (1995).
[17] N. Hatakenaka, M. Shiobara, Ken-ichi Matsuda, and S. Tanda, Phys. Rev. B **57**, 2003 (1998).
[18] S. V. Zaitsev-Zotov, Phys. Rev. Lett. **71**, 605 (1993).
[19] S. V. Zaitsev-Zotov, Phys. Rev. Lett. **72**, 587 (1994).
[20] S. V. Zaitsev-Zotov, G. Remenyi, and P. Monceau, Phys. Rev. B **56**, 6388 (1997).
[21] A. Davidson, B. Dueholm, B. Kryger, and N. F. Pedersen, Phys. Rev. Lett. **55**, 2059 (1985).
[22] A. V. Ustinov, T. Doderer, R. P. Huebener, N. F. Pedersen, B. Mayer, and V. A. Oboznov, Phys. Rev. Lett. **69**, 1815 (1992).
[23] M. G. Castellano, G. Torrioli, C. Cosmelli, A. Costantini, F. Chiarello, P. Carelli, G. Rotoli, M. Cirillo, and R. L. Kautz, Phys. Rev. B **54**, 15417 (1996).
[24] T. Kato and M. Imada, J. Phys. Soc. Jpn. **65**, 2963 (1996).
[25] A. V. Ustinov, B. A. Malomed, and E. Goldobin, Phys. Rev. B **60**, 1365 (1999).
[26] For example, see Ref. 6.
[27] S. Coleman, Phys. Rev. D **15**, 2929 (1977).
[28] C. G. Callan and S. Coleman, Phys. Rev. D **16**, 1762 (1977).
[29] S. Coleman, in *The Whys of Subnuclear Physics*, edited by A. Zichichi (Plenum, New York, 1985), p. 805.
[30] H. A. Kramers, Physica (Utrecht) **7**, 284 (1940).
[31] M. Yumoto, H. Fukuyama, H. Matsukawa, and N. Nagaosa, J. Phys. Soc. Jpn. **68**, 170 (1999).
[32] M. Yumoto, H. Fukuyama, H. Matsukawa, and N. Nagaosa,

Physica B **284-288**, 1667 (2000).
[33] M. Yumoto, H. Fukuyama, H. Matsukawa, and N. Nagaosa, J. Phys. Soc. Jpn. **69**, 2953 (2000).
[34] T. Kato, J. Phys. Soc. Jpn. **69**, 2735 (2000).
[35] D. W. McLaughlin and A. C. Scott, Phys. Rev. A **18**, 1652 (1978).
[36] Y. S. Kivshar and B. A. Malomed, Rev. Mod. Phys. **61**, 763 (1989).
[37] B. I. Ivlev and V. I. Mel'nikov, Phys. Rev. B **36**, 6889 (1987).
[38] U. Weiss, *Quantum Dissipative Systems* (World Scientific, Singapore, 1993).
[39] J. S. Langer, Ann. Phys. (N.Y.) **41**, 108 (1967).
[40] J. S. Langer, Ann. Phys. (N.Y.) **54**, 258 (1969).
[41] I. Affleck, Phys. Rev. Lett. **46**, 388 (1981).
[42] H. Grabert and U. Weiss, Phys. Rev. Lett. **53**, 1787 (1984).
[43] A. I. Larkin and Yu. N. Ovchinnikov, Zh. Éksp. Theor. Fiz. **86**, 719 (1984) [Sov. Phys. JETP **59**, 420 (1984)].